Chapter 8

Correlation between Thermal and Electrical Properties of Spark Plasma Sintered (SPS) Porous Copper

Yaniv Gelbstein, Yedidia Haim, Sergei Kalabukhov, Vladimir Kasiyan, S. Hartmann, S. Rothe and Nahum Frage

Additional information is available at the end of the chapter

http://dx.doi.org/10.5772/59010

1. Introduction

Spark Plasma Sintering (SPS) is a consolidation approach, in which pulsed direct current passes through a graphite die and a compacted specimen, and enabling very high heating rates with simultaneously applying an external pressure. The combination of internal heating and external pressure provides the conditions for fast sintering. SPS parameters have to be determined based on the thermal and electrical properties of the consolidated material, which, evidently, depend on the compact porosity that decreases during the sintering process. In the present study, the effect of porosity of the SPS-processed Cu specimens on their thermal and electrical properties at room temperature was theoretically and experimentally investigated.

There are some theoretical approaches, which may be applied for analysis of transport properties of a porous material. One of the approaches, the "so-called" general effective media (GEM) method (eq. 1) was discussed in [1, 2].

$$x_1 \cdot \frac{\left(\sigma_1,\kappa_1\right)^{1/t} - \left(\sigma_{eff},\kappa_{eff}\right)^{1/t}}{\left(\sigma_1,\kappa_1\right)^{1/t} + A\cdot\left(\sigma_{eff},\kappa_{eff}\right)^{1/t}} = \left(1-x_1\right)\frac{\left(\sigma_{eff},\kappa_{eff}\right)^{1/t} - \left(\sigma_2,\kappa_2\right)^{1/t}}{\left(\sigma_2,\kappa_2\right)^{1/t} + A\cdot\left(\sigma_{eff},\kappa_{eff}\right)^{1/t}} \quad (1)$$

The GEM equation (eq. 1) is usually employed for calculating the effective electrical and thermal conductivities (σ_{eff} and κ_{eff}, respectively) for two-phase materials using the electrical (σ_1 and σ_2) and thermal (κ_1 and κ_2) properties of each phase. The morphological (or geometrical)

parameters (A and t) may be derived from the equation of conductivity percolation [1] or by appropriate modeling of experimental results. The x_1 and (1-x_1) values are the volume fractures of the phases in a two-phase material.

Generally, A and t values depend on the phases distribution and their morphology within two-phase materials. Let us consider a composite material, which consists of continuous matrix and homogenous distributed particles with high aspect ratio (for instance, fibers) of a second phase. For this kind of distribution t value is equal to 1 [1] and the so-called "parallel" and "series" alignment of the particles (relative to the electrical potential or temperature gradients) may be considered. The parameter A varies from ∞ for the parallel to 0 for series alignments. Recently [1], the GEM equation and measured transport properties were successfully used for estimating the fracture and distribution of Sn phase, which displays a fiber shape particles, in the Sn_xTe_{1-x} inter-metallic matrix.

Ke-Feng Cai et al. [3] reported the results of prediction of effective thermal conductivity of porous Al-doped SiC ceramics using the Landauer's expression (eq. 2) derived for spherical and homogeneously dispersed second phase [4].

$$\kappa_{eff} = \kappa_1 \left(\frac{3x_1 - 1}{2} \right) \tag{2}$$

It may be shown that this equation may be derived from the GEM equation (1) if one takes into account that A=2 and t=1.

Another commonly used approach, yet not straightforward for multi-phased materials, to correlate effective transport properties (thermal and electrical conductivity) of porous materials is based on the Weidemann-Franz relation.

$$\kappa_{eff} = L \cdot \sigma_{eff} \cdot T \tag{3}$$

Where, the coefficient L is known as Lorenz number and T represents the absolute temperature. The Lorenz number is constant only in the case when the conduction electrons are scattered elastically. This condition requires that the temperature-independent electron scattering by impurities will dominate over the electron scattering by phonons [5]. These conditions may be achieved at high temperatures or at very low temperatures, where the residual resistivity is predominant. At intermediate temperatures, the condition of elasticity no longer holds and the Lorenz number decreases considerably from the Sommerfeld value. In order to get a better understanding of the L number, let us consider the general expression for L, derived from the Fermi-Dirac statistics (eq. 4) [6] and graphically presented in Fig. 1 for two different electron scattering mechanisms (or scattering parameters, r): by ionized impurities (using scattering parameter r of 3/2) and by acoustic phonons (r=-1/2).

http://dx.doi.org/10.5772/59010

$$L = \left(\frac{k}{e}\right)^2 \left[\frac{\left(r+\frac{7}{2}\right)\left(r+\frac{3}{2}\right)F_{r+5/2}(\eta)F_{r+1/2}(\eta) - \left(r+\frac{5}{2}\right)^2 F^2_{r+3/2}(\eta)}{\left(r+\frac{3}{2}\right)^2 F^2_{r+1/2}(\eta)} \right] \quad (4)$$

Where, e, k, F_r and η are the electrons charge, Boltzmann constant, Fermi integral (defined by eq. 5) and the reduced Fermi energy (E_F/kT), respectively.

$$F_r = \int_0^\infty \xi^r f_o(\eta) \cdot \partial\xi \quad (5)$$

$$f_o(\eta) = \frac{1}{1+\exp(\xi-\eta)} \quad (6)$$

In the expression for F_r (eq. 5)-f_o (defined in eq. 6) and ξ are the Fermi distribution function and the kinetic energy of a charge carrier, respectively.

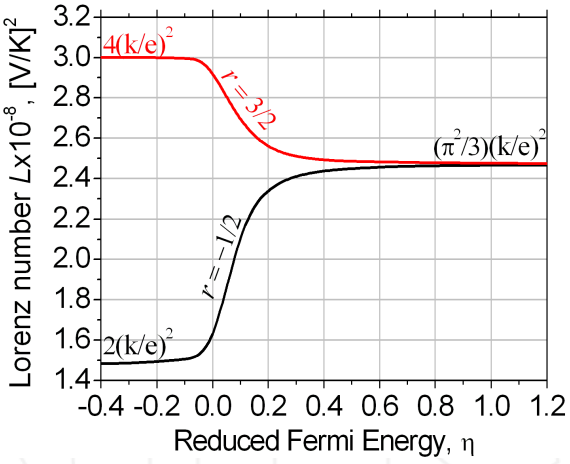

Figure 1. Lorenz number variation with the reduced Fermi energy ($\eta=E_F/kT$) for two different electron scattering mechanisms, by ionized impurities (using scattering parameter r of 3/2) and by acoustic phonons (r=-1/2).

According to this analysis, for materials with low carrier concentrations (η<-0.4), L values reach the classical (Boltzmann statistics) values of $4(k/e)^2$ and $2(k/e)^2$ for ionized impurities and acoustic phonons scattering, respectively. For degenerate materials (η>1.2) L reaches the Sommerfeld value, derived from eq. 7, regardless the scattering mechanism.

$$L = \frac{\pi^2}{3}\left(\frac{k}{e}\right)^2 \tag{7}$$

For the intermediate η values, *L* exhibits a strong dependence on both Fermi energy and the scattering mechanism.

Since Cu is highly conductive metal, the value of η at room temperature may be calculated using eq. 8 and the physical properties of Cu (effective mass, $m^*=1.01m_o$ [7], and carrier concentration, $n=8.4\text{x}10^{22}$ cm^{-3} [8]). The estimated η value is equal to 270 and corresponds to the energetic range where the constant Sommerfeld value valids.

$$n = \frac{8}{3\sqrt{\pi}}\left(\frac{2\pi m^* kT}{h^2}\right)^{3/2}\eta^{3/2} \tag{8}$$

Nevertheless, the Lorenz number differs slightly from the Sommerfeld value due to the inelastic electrons scattering.

The simple consideration presented above shows that for the applying the Weidemann-Franz relation between the transport properties of materials, the specific Lorenz number has to be determined.

It was shown [9], for instance, that Lorenz number of copper alloys depends on their purity and thermo-mechanical treatments. Moreover, in [10] it was established that the Lorenz number for copper films depends on its thickness. This effect was partly attributed to scattering of electrons at the films surfaces and partly to scattering by frozen-in structural defects.

This explanation is based on a distinction between the free paths of electrons for the electrical conductivity process and those for the thermal conductivity process. Being more specific, in a metal, an electric field or a temperature gradient causes an electron drift, which is restricted only by the collisions of the electrons with lattice imperfections (static defects or lattice vibrations). When the electron distribution function is disturbed from its equilibrium value, the rate of return to equilibrium may be expressed by collision processes, which are usually expressed in terms of a relaxation time. Only in case that the relaxation time is the same for both electrical and thermal transport, eq. 7 can be used. This equation is based on the assumption that *L* is a constant independent of the band structure or the relaxation time. Regarding relaxation, it was pointed out in [11] that equilibrium can be reached in two ways: either by processes changing the direction of motion of an electron but not changing its energy significantly, or by processes changing its energy but not the direction – the so-called "horizontal" or "vertical" movements on the Fermi surface. Since the "vertical" movement was found as ineffective in producing electrical resistance, the relaxation times for electrical and thermal conduction are equal only in case that the "vertical" movement is absent. The effective scattering by phonons at high temperatures and by impurities at low temperatures is elastic,

http://dx.doi.org/10.5772/59010

leading to similar relaxation time for the different transport properties. This is the reason for the validity of eq. 7 at very low or high temperatures.

Koh et al. [12] had used a modified Weidemann-Franz relation (eq. 9), which takes into account also the lattice component of the thermal conductivity, for analysis of porous stainless steel and Cu based alloys.

$$\kappa_0 = L\frac{T}{\rho_0} + b \tag{9}$$

Where, ϱ_0 and κ_o are the electrical resistivity and the thermal conductivity of the alloys, respectively, and b is the lattice component of the thermal conductivity.

It was established that for highly conductive materials, such as copper alloys, where the lattice component of the thermal conductivity is relatively small compared to the electronic one, the dependency of the thermal conductivity on T/ϱ for various porosity levels was characterized by a straight curve with a slope L and intercept b. In this case the L and b values depend on the nature of metal only. For stainless steel, for which the lattice and the electronic components are comparable, b value depends on the porosity and specific curve for each porosity level was obtained.

It can be concluded that special care should be taken while using the Weidemann-Franz relation for porous or other multi-phased materials. On the other hand, applying the GEM approach is much more straightforward, giving additional information about the phases' alignment and distribution characteristics

In the presence study, the GEM and Weidemann-Franz relations were applied for investigation of the experimental transport properties results of porous SPS-processed Cu specimens.

2. Experimental

Pure (99.9%) copper powder with a nearly spherical particles shape and an average particle size of about 8μm was consolidated by SPS apparatus (FCT Systems GmbH, Germany) under argon atmosphere with heating and cooling rates of 50°C/min. The specific parameters of the SPS process are presented in Table 1. The porosity of the sintered specimens, (measured by the Archimedes method) was varied in the 0-30 vol.% range.

The microstructure was characterized by optical microscope *Zeiss* (Germany). Electrical resistivity was measured at room temperature by a four-probe method using 1V/50 Hz alternating power source and *Keithley 2182A Nanovoltmeter*. The thermal conductivity was tested at room temperature using the flash diffusivity method (*LFA 457, Netzsch*). Thermal conductivity (κ_{eff}) values were calculated using the equation $\kappa_{eff}=\alpha\, \varrho\, C_p$ where, α is the thermal diffusivity, C_p is the specific heat (measured using differential scanning calorimetry, *STA 449-Netzsch*), and ϱ is the bulk density of the sample.

Porosity, vol%	Temperature, °C	Holding time, min.	Applied uniaxial pressure, MPa
0	700	15	97
1	600	15	97
10	400	2	88
15	400	2	70
20	400	2	53
30	400	2	35

Table 1. Spark Plasma Sintering conditions and porosity of the specimens.

The thermal conductivity measurements were conducted under ~1atm argon, similarly to the SPS conditions.

3. Results

The microstructure of the porous Cu speciemns is shown in Fig. 2.

The average grain size of about 7-8μm indicates no coarsening effects during the SPS process. The pores are homogenously distributed within the metallic matrix.

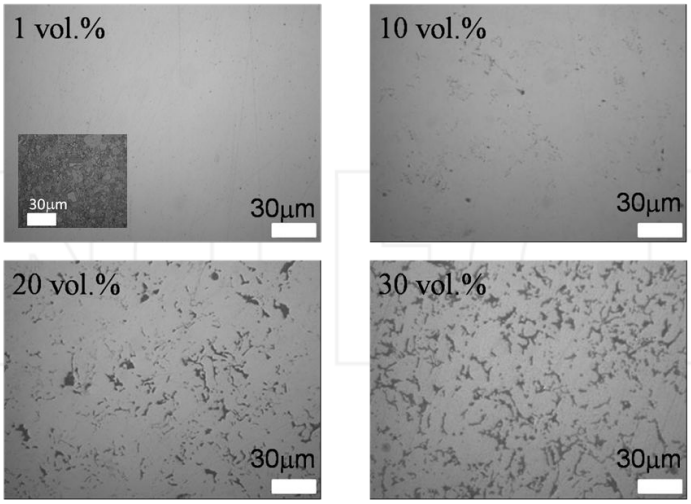

Figure 2. Optical images of the SPS-processed specimens. The microstructure of the almost dense specimen (1vol% porosity) after etching was presented as the insert in the corresponded image.

http://dx.doi.org/10.5772/59010

Values of the electrical resistivity and thermal conductivity measured at room temperature as a function of porosity are shown in Fig. 3.

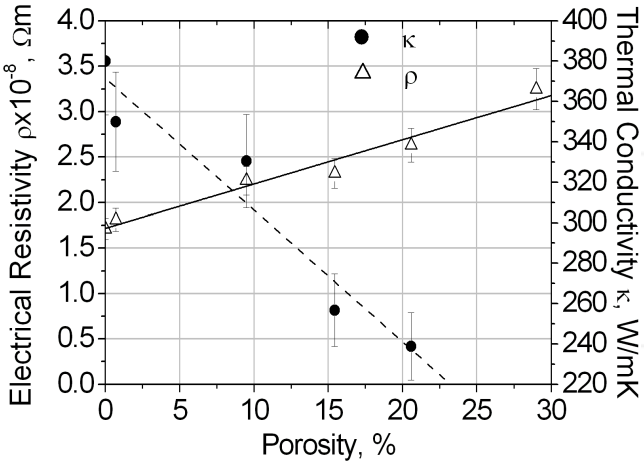

Figure 3. The electrical resistivity and thermal conductivity of porous Cu specimens.

As was expected, a general trend of increasing the electrical resistivity and decreasing the thermal conductivity values with increasing of the porosity amount was observed. Furthermore, additional insights regarding the geometrical alignment and porous distribution can be obtained, upon applying the GEM and the Weidemann-Franz equations.

4. Discussion

In order to apply the GEM equation (1) and Weidemann-Franz relation (eq. 3) for analyzing the experimental results presented in Fig. 3, the thermal and electrical conductivities of pure Cu and argon, which filled the micrometric pores, have to be determined. The thermal and electrical conductivities of pure copper (κ_1 and σ_1, respectively, in eq. 1) are reported in [13, 14]. For argon, the electrical conductivity, σ_2, is negligible, while the thermal properties has to be discussed. According to [15], at normal conditions, heat convection through a porous metallic structure becomes of practical importance only at temperatures above 1000K and for pore diameter larger than 5000μm. It was also reported in [15] that heat transfer by radiation in the pores at moderate and high temperatures might be neglected. Thus, for materials with relatively small pores, as in our case, conductive heat transfer is the dominant process at the investigated temperature.

Under normal pressure, the thermal conductivity of Ar [16, 17] may be calculated according to eq.10

$$\kappa_{Ar} = 1.47 \cdot 10^{-5} \frac{T^{1/2}}{1 + 142/T} \quad \left[Watt / cmK \right] \tag{10}$$

and is equal to ~1.73x10^{-2} W/mK at room temperature.

4.1. General Effective Media (GEM) theory

The aims of this paragraph is to confirm that the effective transport properties of the porous material may be calculated using one set of the geometrical parameters *A* and *t*. We started with the analysis of the measured values of the effective transport properties for the specimen showing a 20 vol.% porosity. By solving together two equations, based on the GEM approach, for the thermal and electrical conductivities, the values *A*=1.3 and *t*=1 were obtained. These values were used for calculation of the transport properties for the entire investigated specimens, showing various porosity amounts. A very good agreement was found between the calculated and experimental results, as can be seen in Figs. 4-5, while comparing the experimental data to various calculated curves with different *A* values. The experimental points are located between the curves corresponded to *A* values in the range of 1÷2. Thus, we may conclude that the pores are homogeneously dispersed and have nearly spherically shaped, in agreement with the micro-structural observations (Fig. 2).

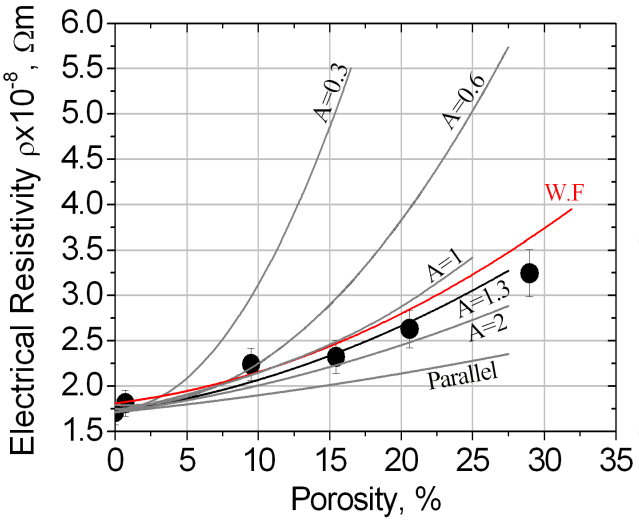

Figure 4. Effective electrical resistivity (=σ_{eff}^{-1}) values for the investigated porous Cu samples, calculated by the GEM equation substituting *A* and *t* parameters of 0.3,1; 0.6,1; 1.3,1; 2,1 and ∞,1 (parallel alignment); and by the Weidemann-Franz (W.F.) relation. The experimentally measured results are shown by the black points.

http://dx.doi.org/10.5772/59010

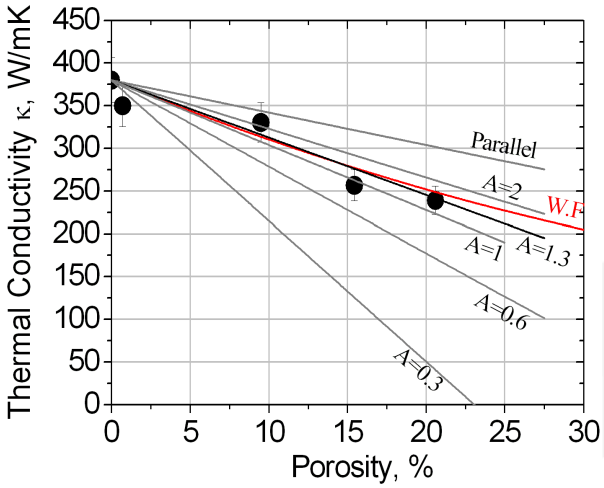

Figure 5. Effective thermal conductivity (κ_{eff}) values for the investigated porous Cu samples, calculated by the GEM equation substituting *A* and *t* parameters of 0.3,1; 0.6,1; 1.3,1; 2,1 and ∞,1 (parallel alignment); and by the Weidemann-Franz (W.F.) relation. The experimentally measured results are shown by the black points.

4.2. Weidemann-Franz (W.F.) relation

The calculated values of the transport properties as a function of the porosity levels using Weidemann-Franz relation (eq. 3) are also presented in Figs 4-5. The calculations took into account the Lorenz number for Cu at 0°C (2.23×10^{-8} $[V/K]^2$) reported in [18]. This value is slightly differs from the Sommerfeld value of 2.47×10^{-8} $[V/K]^2$ (derived from eq. 7), which is commonly used for highly degenerated materials. Nevertheless, there is a good agreement between the calculated and the experimental results for both the electrical resistivity and the thermal conductivity values.

4.3. W.F. vs. GEM

While comparing the two suggested approaches for estimating the electrical and thermal transport properties of porous materials, several general guidelines can be obtained:

1. Applying the GEM approach upon measurement of κ_{eff} and σ_{eff} (or ϱ_{eff}) of one known porosity level, and previous knowledge of the same properties of the matrix phase, can give a good approximation for the porosity amount dependency of the electrical and thermal conductivities for any given porosity amount in addition to some insight about the porosity alignment, distribution and morphology. It should be remembered that, a special care should be taken upon using any approximation such as eq. 2, since dependent on the powdering approach and the crystallographic nature of the matrix composition, the porosity morphology do not have to be spherical with an isotropic distribution.
2. Applying the Weidemann-Franz relation (equation 3) for a metallic or highly degenerated porous material, using the Sommerfeld value of *L* (derived from eq. 7) at moderate

temperatures (e.g. room temperature) leads to inaccurate estimations due to inelastic scattering effects. Therefore, measurement of both κ_{eff} and σ_{eff} (or ϱ_{eff}) for one known porosity level, for evaluation of *L*, should not be avoided. For less conductive matrix materials, phonons thermal conductivity effects are involved, which are expected to vary with the porosity amount. For semiconductors with reduced Fermi energy in the range of $-0.4<\eta<1.2$, *L* depends also on the scattering mechanism and the Fermi energy. For semiconductors or insulators with $\eta<-0.4$, *L* depends on the scattering mechanism as well. Such an approach can't supply any insight on the geometrical alignment and morphology of the pores.

5. Conclusions

The thermal and electrical conductivities for spark plasma sintered porous Cu samples were experimentally measured at room temperature and theoretically correlated to the GEM and Weidemann-Franz relations. Both of the theoretic approaches showed a good agreement to the experimental values. Yet several restrictions were discussed upon generalizing the proposed theoretical procedures for any porous material. Applying the GEM equation was found as the ideal approach for estimating the thermal and electrical characteristics of porous materials, due to the possibility to give a good approximation for the porosity amount dependency of the electrical and thermal conductivities for any given porosity amount in addition to some insight about the porosity alignment, distribution and morphology.

Acknowledgements

The authors wish to acknowledge Mr. Yair George for his assistance in the experimental measurements.

Author details

Yaniv Gelbstein[1*], Yedidia Haim[2], Sergei Kalabukhov[1], Vladimir Kasiyan[1], S. Hartmann[3], S. Rothe[3] and Nahum Frage[1]

*Address all correspondence to: yanivge@bgu.ac.il.

1 Department of Materials Engineering, Ben-Gurion University of the Negev, Israel

2 Department of Mechanical Engineering, Ben-Gurion University of the Negev, Israel

3 Institute of Applied Mechanics, Clausthal University of Technology, Clausthal-Zellerfeld, Germany

References

[1] Yaniv Gelbstein, "Thermoelectric Power and Structural Properties in Two Phase Sn/SnTe Alloys", Journal of Applied Physics 105, 023713 (2009).

[2] Maclachlan, D.S., Blaszkiewicz, M. &Newnham, R.E. *J Am Ceram Soc*73(8), 2187-2203 (1990).

[3] Ke-Feng Cai, Jin-Ping Liu, Ce-Wen Nan, Xin-Min Min, "Effect of porosity on the thermal-electric properties of Al-doped SiC ceramics", Journal of Materials Science Letters 16 (1997) 1876-1878.

[4] Rolf Landauer, "The Electrical Resistance of Binary Metallic Mixtures", Journal of Applied Physics Vol. 23, No. 7, p.779 (1952).

[5] R. W. Arenz, C. F. Clark, and W. N. Lawless, "Thermal conductivity and electrical resistivity of copper in intensemagnetic fields at low temperatures", Physical Review B Vol. 26, No. 6, p. 2727 (1982).

[6] Y. Gelbstein, Z. Dashevsky and M.P. Dariel, "High performance *n*-type PbTe-basedmaterials for thermoelectric applications", Physica B 363 196-205 (2005).

[7] Arthur Beiser, "Perspectives of Modern Physics", Mc-Graw-Hill International Editors, p.487 (1969).

[8] Edward Ramsden, "Hall-Effect Sensors – Theory and Applications", 2nd Edition, Elsevier, p. 8 (2006).

[9] Robert L. Powell, Hans M. Roder, and William J. Hall, "Low-Temperature Transport Properties of Copper and Its Dilute Alloys: Pure Copper, Annealed and Cold-Drawn", Physical Review Vol. 115, No. 2, p. 314 (1959).

[10] Prem Nath and K. L. Chopra, "Thermal Conductivity of Copper Films", *Thin Solid Films, 20* (1974) 53-62.

[11] G. K. White and R. J. Tainsh, "Lorenz Number for High-Purity Copper", Physical Review Vol. 119, No. 6, p.1869 (1960).

[12] J. C. Y. Koh and Anthony Fortini, "Prediction of Thermal Conductivity and Electrical Resistivity of Porous Metallic Materials", Int. J. Heat Mass Transfer Vol. 16, pp. 2013 (1973).

[13] R.P. Tye, "Thermal Conductivity", vol. 2, p.147, Academic Press (1969).

[14] Donald R. Askeland, "The Science and Engineering of Materials", 3rd edition, p. 597, PWS Publishing Company (1989).

[15] R. Zabbarov, "Effect of Porosity and Treatment on the Thermal Conductivity of Cermets", Journal of Engineering Physics 213 (1967), *(translated from: Inzhenerno-Fiziheskii Zhurnal, Vol. 13, No. 3, pp. 373-375, 1967).*

[16] Saul Dushman, "Scientific Foundations of Vacuum Technique", 2nd edition, pp. 40, 42, John Wiley & Sons inc. (1962).

[17] D.W. Stops, "The Mean Free Path of Gas Molecules in the Transition Regime", J. Phys. D: Appl. Phys. 3 685 (1970).

[18] N.F. Mott and H. Jones, "The Theory of the Properties of Metals and Alloys", Oxford University Press, p.307 (1958).

INTECH